Nonlinear Elastic Multi-Path Reciprocal Method for Damage Localisation in Composite Materials

S. Boccardi, D.B. Callá, F. Ciampa, M. Meo

Department of Mechanical Engineering, University of Bath, Bath BA2 7AY, UK

Abstract

Nonlinear ultrasonic techniques rely on the measurement of nonlinear elastic effects caused by the interaction of ultrasonic waves with the material damage, and have shown high sensitivity to detect micro-cracks and defects in the early stages. This paper presents a nonlinear ultrasonic technique, here named *nonlinear elastic multi-path reciprocal* method, for the identification and localisation of micro-damage in composite laminates. In the proposed methodology, a sparse array of surface bonded ultrasonic transducers is used to measure the second harmonic elastic response associated with the material flaw. A reciprocal relationship of nonlinear elastic parameters evaluated from multiple transmitter-receiver pairs is then applied to locate the micro-damage. Experimental results on a damaged composite panel revealed that an accurate damage localisation was obtained using the normalised second order nonlinear parameter with a high signal-to-noise-ratio (~11.2 dB), whilst the use of bicoherence coefficient provided high localisation accuracy with a lower signal-to-noise-ratio (~1.8 dB). The maximum error between the calculated and the real damage location was nearly 13 mm. Unlike traditional linear ultrasonic techniques, the proposed *nonlinear elastic multi-path reciprocal* method allows detecting material damage on composite materials without a priori knowledge of the ultrasonic wave velocity nor a baseline with the undamaged component.

Keywords

Composite Materials, Structural Health Monitoring (SHM), Nonlinear Damage Localization.

1. Introduction

In the last decade, carbon fibre–reinforced plastic (CFRP) composite materials have been increasingly used in different sectors, from aerospace to automotive and civil, due to their good in-plane mechanical and lightweight properties. However, composites are susceptible to low velocity impacts that can generate barely visible impact damage (BVID), micro-cracks and delamination, which can irreparably affect the integrity of the structure. In particular, if the impact occurs at very low velocity, damage can be a mixture of splitting between fibres, matrix cracking, fibres fracture and internal delamination due to inter-laminar shear and tension. These damaged modes weaken the mechanical properties of the structure and can be completely invisible when viewed from the external impacted surface. Hence, both linear and nonlinear ultrasonic structural health monitoring (SHM) techniques based on sparse transducer arrays have been developed in the last few years to provide an early warning and increase of safety of composite components [1-6]. Linear beamforming techniques, such as the statistical maximum-likelihood estimation [7] and the reconstruction algorithm for probabilistic inspection of damage (RAPID) [8] have shown a high level of accuracy for the detection and localisation of damage in composites. However, linear ultrasonic techniques typically rely on the measurement of wave scattering and reflections, as well as changes of macroscopic elastic features caused by the presence of damage such as wave attenuation and group velocity. Hence, these methodologies may lack of sensitivity to micro-flaws due to low acoustic impedance mismatch at damage location. Moreover, linear ultrasonic methodologies with sparse transducer arrays require the

knowledge of waveforms associated to the undamaged component, which is generally difficult to obtain.

On the other hand, ultrasonic waves propagating in a damaged structure at a particular driving frequency can generate "clapping" motion of the region normal to the crack interfaces or nonlinear friction (rubbing) between the defect surfaces excited by small tangential stresses. This result in the creation of nonlinear elastic effects such as higher harmonics and sub-harmonics of the excitation frequency, which can be used as signature for micro-damage detection. A number of authors have recently focused their studies on the nonlinear behaviour of ultrasonic waves in composites, both numerically and experimentally [9, 10]. Typically, both the second and third order nonlinear elastic responses are used for material damage identification and localisation [11]. Ciampa et al. [12, 13] and Malfense-Fierro and Meo [14] use the second order harmonic response and nonlinear inverse filtering technique in order to detect damage in multi-layered media.

This paper presents a novel in-situ nonlinear ultrasonic approach, here called nonlinear elastic multi-path reciprocal (NEMR) method, for the localisation of micro-damage in composite components. A sparse array of surface bonded ultrasonic transducers is here used to measure the second harmonic nonlinear elastic response associated with the material damage by means of the normalised classical second order nonlinear coefficient and the bicoherence parameter. The micro-damage localisation is then achieved by analysing the reciprocal relationship of these nonlinear coefficient calculated from multiple transmitter-receiver pairs. The paper is outlined as follows: in Section 2 there is an introduction to the nonlinear parameters involved; in Section 3 the NEMR technique is explained in detail; Section 4 shows the experimental set-up; in

Section 5 it is possible to read the experimental results; in Section 6 the main conclusions are discussed.

2. Nonlinear Parameters

According to Section 1, both micro-cracks and delamination, when excited by ultrasonic waves can generate nonlinear material responses. These elastic effects can be analytically modelled by using the classical nonlinear elasticity (CNE) theory [15]. Assuming a one-dimensional longitudinal wave propagation along the x-direction, the elastodynamic wave equation [16] can be expressed as the power series of the strain $\varepsilon_x = \partial u(x,t)/\partial x$ as follows

$$\rho \frac{\partial^2 u(x,t)}{\partial t^2} = \frac{\partial \sigma}{\partial x} = (\lambda + 2\mu)\left[\frac{\partial}{\partial x}\left(1 + \beta\varepsilon_x + \delta\varepsilon_x^2\right)\varepsilon_x \right] \tag{1}$$

where σ is the stress and β and δ are second and third order elastic coefficients, respectively. The second order nonlinear parameter β is typically two or three order of magnitude higher than γ and it can be used as a reliable signature for damage detection. Equation (1) is generally solved via a perturbation theory that leads to the following expression of the nonlinear parameter β:

$$\beta = \frac{8A_2}{A_1^2 x k^2}. \tag{2}$$

In Eq. (2), A_1 and A_2 are the fundamental and the second harmonic amplitudes, respectively, k is the wave number and x is the propagation distance of the propagating waveform from the nonlinear source (i.e. damage location). The second order nonlinear parameter β is a material property (it is constant all over the material) and its formulation [Eq. (2)] is obtained by assuming no material attenuation. To overcome this limitation, in this paper a normalised version of β is used, here defined as $\overline{\beta}$, which

is only function of the fundamental and second harmonic amplitudes and may change from point to point within the medium, with the highest value at the damage location. This new normalised second order nonlinear coefficient $\overline{\beta}$ is defined as follows:

$$\overline{\beta} = \frac{A_2}{A_1} = \sqrt{\frac{|P(2\omega_1)|}{|P(\omega_1)|}} \tag{3}$$

where $|P(\omega_1)|$ and $|P(2\omega_1)|$ are the magnitudes of the power spectral densities associated with the fundamental angular frequency ω_1 and the second harmonic angular frequency $2\omega_1$. However, $\overline{\beta}$ relies on magnitude ratios and discards all phase information contained in the acquired waveforms. Higher order statistics (HOS), such as the bispectral analysis, are a valid alternative to the second order nonlinear coefficient as they can be used to measure both the magnitude and phase of the higher order harmonic frequency components [17]. Particularly, the bispectrum B is the two-dimensional Fourier Transform of the third order correlation function and, for a real, zero-mean stationary random process $s(t)$, it is given by:

$$B(\omega_m, \omega_n) = \int_{-\infty}^{+\infty} \int_{-\infty}^{+\infty} R_{sss}(\tau_1, \tau_2) e^{j(\omega_m \tau_1 + \omega_n \tau_2)} d\tau_1 d\tau_2 \tag{4}$$

where $R_{sss}(\tau_1,\tau_2)$ is the third order auto-correlation function of $s(t)$. In the frequency domain, Eq. (4) can be rewritten as:

$$B(\omega_m, \omega_n) = E\left[S(\omega_m) S(\omega_n) S^*(\omega_m + \omega_n)\right] \tag{5}$$

where $S(\omega)$ is the Fourier Transform of the measured signal $s(t)$ and the asterisk sign "*" corresponds to a complex conjugate operation. The three frequency components ω_n, ω_m and $\omega_n + \omega_m$ have a special phase relation, called quadratic phase coupling (QPC) [17], which defined as follows:

$$\varphi_m + \varphi_n = \varphi_{m+n} \tag{6}$$

where φ_n and φ_m are the phases of the signal at frequencies ω_n and ω_m, respectively, and φ_{m+n} is the phase of the signal at frequency $\omega_n + \omega_m$. QPC allows the identification of structural nonlinearity by discarding the signal noise that, differently, is not quadratic phase coupled [18]. Similarly to the second order nonlinear parameter β, also the bispectrum B can be replaced by its normalised non-dimensional counterpart, the bicoherence coefficient b^2, which is defined as follows [17]:

$$b^2 = \frac{|B(\omega_1, \omega_1)|^2}{P(\omega_1)P(\omega_1)P(2\omega_1)} \tag{7}$$

with $B(\omega_1,\omega_1) = E\left[S(\omega_1)S(\omega_1)S^*(2\omega_1)\right]$ the bispectrum calculated at the fundamental frequency ω_1. The NEMR damage localisation technique will use either the coefficient $\overline{\beta}$ or b^2 as input and is reported in next Section.

3. Nonlinear Multi-Path Reciprocal (NEMR) method

The NEMR method allows the estimation of damage location on composite panels. A number N of ultrasonic sensors is surface bonded on a composite plate-like structure with impact damage. The NEMR technique is based on the assumption that the closer the receiving sensor is to damage, the higher will be the acquired second order nonlinear response. Hence, a reciprocal relationship is here introduced in order to retrieve the closest point to damage along the path between multiple transmitter-receiver pairs.

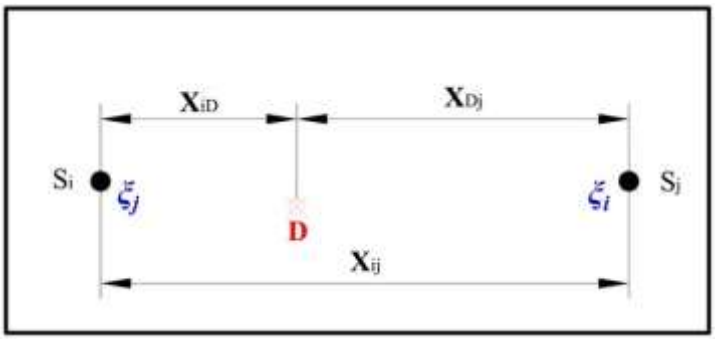

Figure 1 - Scheme for a couple of sensors and relative wave path.

According to Figure 1, X_{ij} is the distance between two sensors S_i and S_j, and the sensor-damage distances are X_{iD} and X_{Dj} with i,j = 1, 2, …, N. The reciprocal relationship between each sensor-damage path and the associated ultrasonic nonlinear response is given by:

$$X_{iD} = \frac{X_{Dj}\xi_i}{\xi_j}. \tag{8}$$

In Eq. (8), the parameter ξ was used to identify either the normalised second order nonlinear coefficient $\overline{\beta}$ or the bicoherence b^2. By substituting the total distance X_{ij} in Eq. (8), the distance between the sensor S_i and the point closest to damage, D_{ij}, is:

$$X_{iD} = \frac{X_{ij}\xi_i}{\xi_j + \xi_i} \tag{9}$$

Similarly, the reciprocal distance between the sensor S_j and the damage is:

$$X_{Dj} = \frac{X_{ij}\xi_j}{\xi_j + \xi_i}. \tag{10}$$

The transducers-damage distances can be geometrically considered as the radii of circumferences located in a Cartesian reference frame xOy with the origin at the bottom left corner of the panel. The damage location on each single path can be calculated as the intersection point of two tangent circumferences as follows:

$$(x - X_i)^2 + (y - Y_i)^2 = r_{iD}^2 \tag{11}$$

where $r_{iD} = X_{iD}$.

Substituting Eq. (9) into (11), yields:

$$(x - X_i)^2 + (y - Y_i)^2 = \left(\frac{X_{ij}\xi_i}{\xi_j + \xi_i}\right)^2. \tag{12}$$

For each pair of transmitter-receiver transducer, it is now possible to calculate the coordinates x_{Dij} and y_{Dij} associated with the damage location as follows

$$x_{D_{ij}} = x_i - \frac{\xi_i}{\xi_i + \xi_j}\left(x_i - x_j\right), \tag{13a}$$

$$y_{D_{ij}} = y_i - \frac{\xi_i}{\xi_i + \xi_j}\left(y_i - y_j\right). \tag{13b}$$

By finally considering all the possible paths and tangent circumferences between multiple transducers pairs, damage coordinates can be calculated as follows:

$$x_D = \frac{1}{Q}\left[\sum_{\substack{i,j \\ i \neq j}} x_{D_{ij}}\right], \qquad y_D = \frac{1}{Q}\left[\sum_{\substack{i,j \\ i \neq j}} y_{D_{ij}}\right] \tag{14}$$

where $Q = N(N-1)/2$ is the number of possible paths between reciprocal transducers. Figure 2 shows an example of the NEMR image with multiples paths and tangential circumferences for two pairs of transducers.

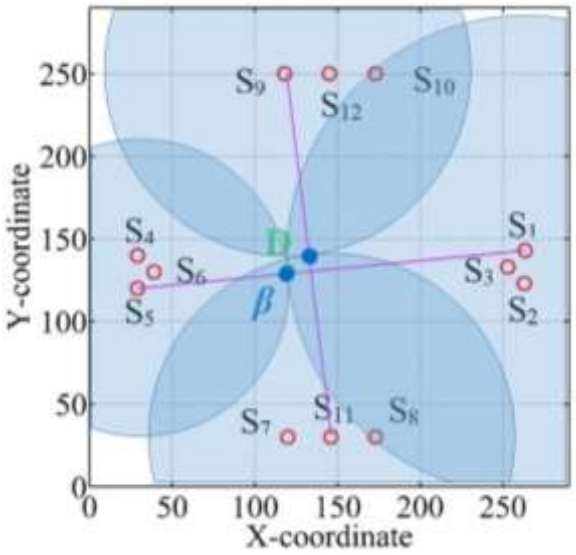

Figure 2 – Example of tangent circumferences in NEMR method for two pairs of transducers.

4. Experimental Set-up

The NEMR algorithm for damage localisation, introduced in Section 3, was experimentally validated on a composite panel with dimensions 290 x 290 x 3 mm,

made of twenty-five layers of prepreg T800-M21 (see Table 1) with a stacking sequence of $[(0/90)_6/\overline{0}]_s$.

Table 1 - M21/T800 prepreg sheet properties.

Properties	**Value**
Young's modulus	E_{11} = 157 GPa
	$E_{22} = E_{33}$ = 8.5 Gpa
Poisson's ratio	ν_{12} = 0.35
Shear modulus	G_{12} = 4.5 Gpa

Table 2 - Piezoelectric sensors coordinates on the composite plate.

Sensor	**x coordinate (mm)**	**y coordinate (mm)**
1	263.5	143
2	263	123
3	253	130
4	29	140
5	29	120
6	39	130
7	120	30
8	173	30
9	118	250
10	173	250
11	146	30
12	145	250
Dam.	120	130

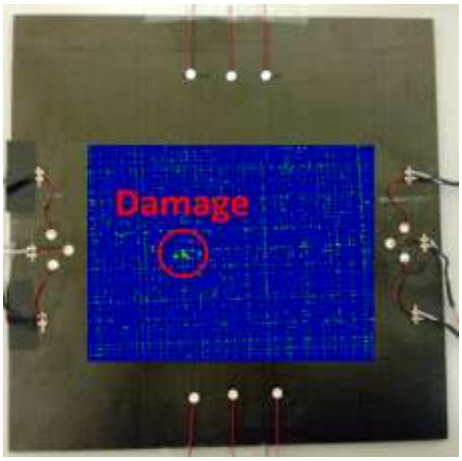

Figure 3 – C-Scan of the panel after impact. Damage is barely visible.

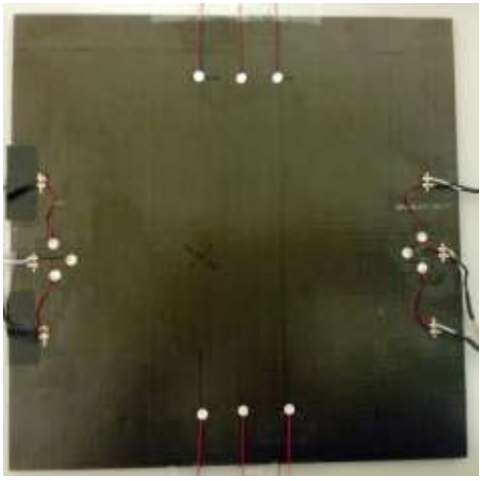

Figure 4 - Composite plate experimental set-up.

In order to obtain barely visible impact damage, a low-velocity impact at the energy of 12 J was applied on the panel (Figure 3). Twelve surface bonded piezoelectric sensors (AmericanPiezo transducers with a central frequency of 330 kHz) were placed on the specimen as shown in Figure 4 and their positions are reported in Table 2. Ultrasonic bursts of 200 cycles were used to excite the specimens at multiple frequencies (Figure 5). The responses of these excitations were then measured with a sampling frequency of 10 MHz. The signal generator (TTI 50 MHz Pulse Generator T6501) was linked to an amplifier (Falco Systems DC 5 MHz High Voltage WMA-300) and the received signals were recorded with a Pico Scope instrument (Pico Technology pc oscilloscope 100V max input, Model 4424). It should be noted that the transmitted frequency plays an important role in NEMR method since the most accurate results are achieved when the damaged region is vibrating so that nonlinear material response is high enough to display harmonic frequencies. The NEMR damage location algorithm was performed using a Matlab code as post-processing manipulation of the recorded signals.

5. Experimental Results

The second order harmonic response was initially found by using an ultrasonic sweep with a frequency range between 150 and 500 kHz and a frequency step of 70 kHz. The highest nonlinear responses were achieved at the fundamental frequencies of 218.5 kHz and 318.95 kHz (Figure 6). These frequencies were then selected to transmit ultrasonic bursts as in Section 4. A representative ultrasonic wave response using a burst input signal is shown in Figure 5.

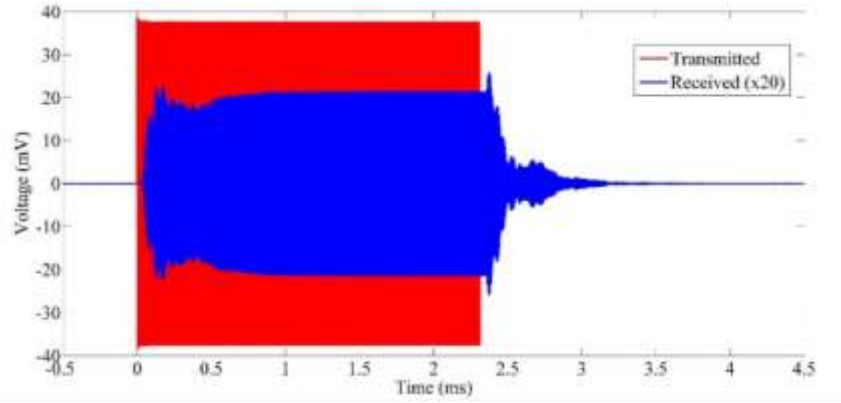

Figure 5 - Ultrasonic burst (red line) sent at 218.5 kHz and received response (blue line).

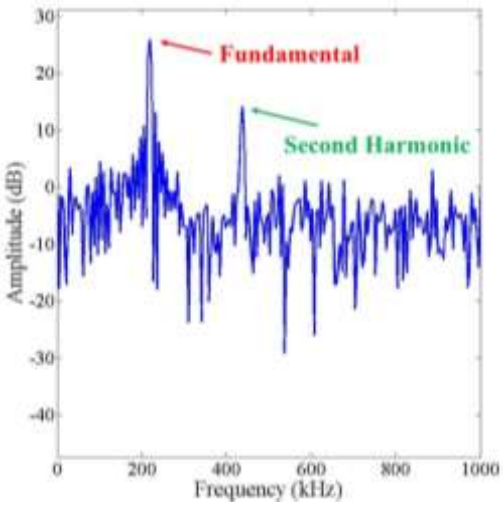

Figure 6a - Spectrum of a received signal (input at a frequency of 218.5 kHz).

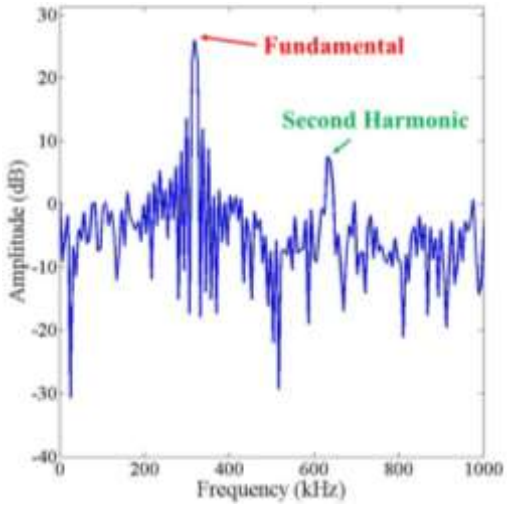

Figure 6b - Spectrum of a received signal (input at a frequency of 318.95 kHz).

The signal-to-noise-ratio (SNR) evaluated in the recorded structural responses at the input frequencies of 218.5 kHz and 318.95 kHz was ~11.2 dB and ~1.8 dB, respectively. SNR, the ratio of the power of the signal (meaningful information) and the power of background noise (unwanted signal), was calculated through the MATLAB function *"snr"*. The error ψ between the calculated and the real damage position was found through the following equation:

$$\psi = \sqrt{\left(x_{real} - x_{calculated}\right)^2 + \left(y_{real} - y_{calculated}\right)^2} \tag{15}$$

The different SNR affected the damage localisation results and it was analysed with the NEMR method. Using the normalised nonlinear second order parameter $\overline{\beta}$ as algorithm input, the most accurate damage localisation was achieved with a SNR of ~11.2 dB at the driving frequency of 218 kHz. Conversely, by using the bicoherence parameter b^2, the most accurate result was achieved in the case of higher noise (SNR = ~1.8 dB) with a driving frequency of 318 kHz. This was in accordance with Section 2 since bicoherence allowed the detection of damage nonlinearities even in the presence of elevated level of noise due to QPC. Hence, according to Eqs. (13a), the damage closest point D_{ij} was calculated on the path between each pair of sensors and two locations were found: one with the $\overline{\beta}$ parameter and the other with the bicoherence b^2, respectively (Figures 6-9).

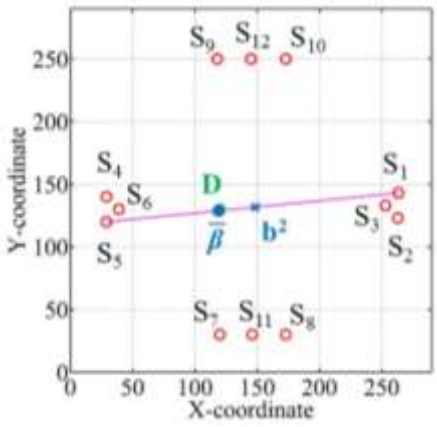

Figure 7 – Reciprocal relationship applied to a horizontal path with a frequency of 218.5kHz.

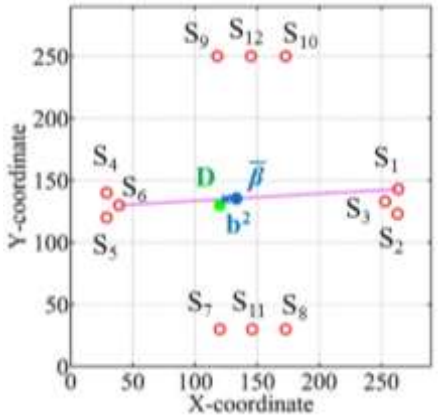

Figure 8 - Reciprocal relationship applied to a horizontal path with a frequency of 318.95 kHz.

Figure 7 shows an example of horizontal path between sensors S_1 and S_5 (hollow circles) where the use of nonlinear parameter $\overline{\beta}$ resulted in a more accurate damage localisation (full dark circles) with an error ψ of nearly 2 mm [see Eq. (15)]. In Figure 8, instead, the bicoherence parameter b^2 was the best option (x signs, ψ ~6 mm). Even when the damage was not located along the straight line between the transmitter and

receiver transducers, as in the vertical paths of Figure 9 and 10, the NEMR technique was able to find the coordinates closest to damage location (i.e. the errors were ~30 mm and ~24 mm, respectively).

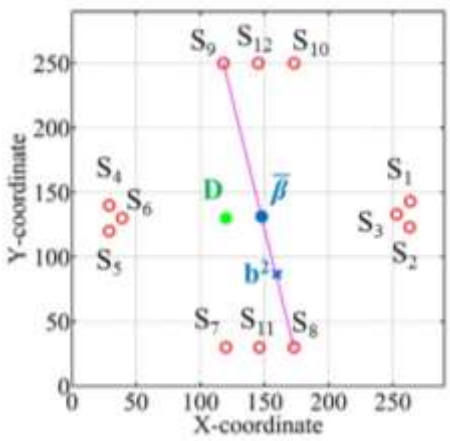

Figure 9 - Reciprocal relationship applied at vertical path n°12 at frequency 218.5 kHz.

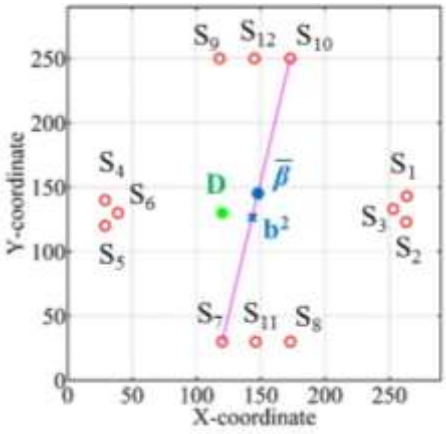

Figure 10 - Reciprocal relationship applied at vertical path n°11 at frequency 318.95 kHz.

Figure 11 shows the results by using 218.5 kHz as transmitting frequency where the closest values to the damaged region were those relative to $\overline{\beta}$.

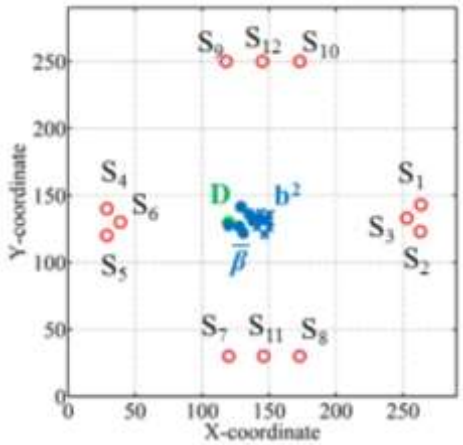

Figure 11 - NEMR best values with 218.5 kHz as transmitting frequency.

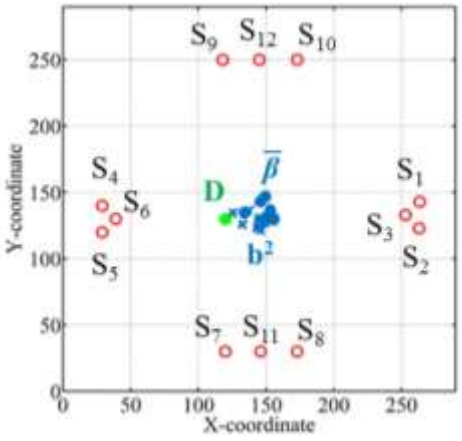

Figure 12 - NEMR best values with 318.95 kHz as transmitting frequency.

In Figure 12, the best results were obtained by considering 318.95 kHz as transmitting frequency and the most accurate damage localisation was achieved through the bicoherence b^2. According to Section 3, once all coordinates were calculated on each single path, Eq. (14) was used to reveal the actual damage location. Eq. (14) was performed a second time excluding the results from the paths in which $d_{Dij} > 3\sigma$ where $d_{Dij} = \sqrt{(x_{Dij} - x_D)^2 + (y_{Dij} - y_D)^2}$ and $\sigma = \sqrt{\frac{1}{Q}\sum_{\substack{i,j \\ i \neq j}} d_{Dij}^{\ 2}}$. Hence, the damage position was identified for all nonlinear responses (see Figure 13 and 14) and the results showed a maximum error of ~13 mm for the frequency of 218.5 kHz with $\overline{\beta}$ and ~14.4 mm for the frequency of 318.95 kHz with b^2. These results are more than satisfactory even though this technique does not use any baseline and does not need a priori knowledge of the wave velocity.

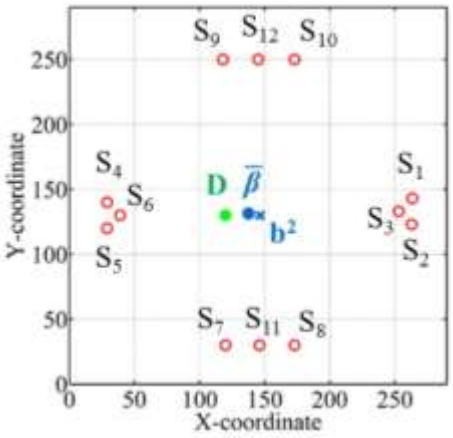

Figure 13 - NEMR method damage positions at frequency 218.5 kHz.

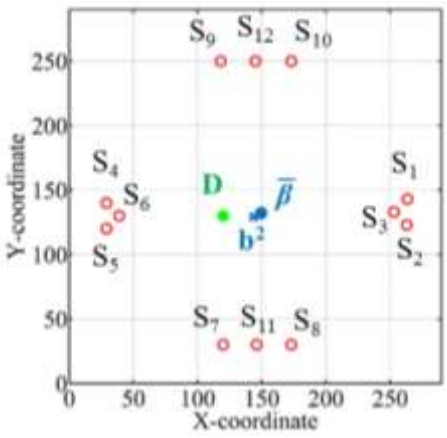

Figure 14 - NEMR method damage positions at frequency 318.95 kHz.

6. Conclusions

In this paper, a novel nonlinear damage localisation technique was presented. It allows damage localisation on composite structures by sending and receiving an ultrasonic

signal from a number of surface bonded sensors placed close to the edge of a panel. Opposite sensors are coupled and the point closest to damage is found on the path between them through a reciprocal relationship involving the nonlinear parameters β and B (see Section 2 and 3). Finally, the damage location is found by considering the calculated positions on every path and discarding the worst cases. The second parameter is more sensitive to nonlinearities since it takes in account the quadratic phase coupling effect at the second harmonic. This information is useful to discriminate the material nonlinear features with respect to both experimental and environmental noise sources. The proposed method was experimentally validated on a damaged anisotropic plate-like structure that presented different fibre orientations, thus various attenuation effects of the original wave with respect to the path angle. During the experimental validation, the two nonlinear parameters were replaced by their corresponding dimensionless coefficients, i.e. the normalised second order nonlinear parameter $\overline{\beta}$ and the bicoherence b^2. Experimental results demonstrated that the anisotropy and different wave attenuations on the structure did not affect damage localisation. Surely, the technique requires a distribution of sending and receiving sensors able to cover the delaminated area. The results showed that an accurate damage localisation was achieved through $\overline{\beta}$ when the SNR was higher (SNR = 11.2 dB at a transmitting frequency of 218.5 kHz) whilst the use b^2 of was useful when the SNR was lower (SNR = 1.8 at a frequency of 318.95 kHz). The maximum error between the calculated and the impact locations was ~13 mm. Since the impact energy in composites produces a delamination all around the impact point, the accuracy of this method can be considered more than satisfactory even though, in contrast to previous damage localisation algorithms, it does not require a priori knowledge of structural lay-up and thickness, as well as group velocities of the propagating waveforms.

7. References

1. Yu, L. and V. Giurgiutiu, *In situ 2-D piezoelectric wafer active sensors arrays for guided wave damage detection.* Ultrasonics, 2008. **48**(2): p. 117-134.
2. Kessler, S.S., S.M. Spearing, and C. Soutis, *Damage detection in composite materials using Lamb wave methods.* Smart Materials and Structures, 2002. **11**(2): p. 269.
3. Mal, A.K., F. Ricci, S. Gibson, and S. Banerjee. *Damage detection in structures from vibration and wave propagation data*. in *NDE for Health Monitoring and Diagnostics*. 2003. International Society for Optics and Photonics.
4. Antonucci, V., M. Ricciardi, F. Caputo, A. Langella, V. Lopresto, V. Pagliarulo, A. Rocco, C. Toscano, P. Ferraro, and A. Riccio, *Non destructive techniques for the impact damage investigation on carbon fibre laminates.* Procedia Engineering, 2014. **88**: p. 194-199.
5. Pagliarulo, V., A. Rocco, A. Langella, A. Riccio, P. Ferraro, V. Antonucci, M. Ricciardi, C. Toscano, and V. Lopresto, *Impact damage investigation on composite laminates: comparison among different NDT methods and numerical simulation.* Measurement Science and Technology, 2015. **26**(8): p. 085603.
6. Riccio, A., F. Caputo, G. Di Felice, S. Saputo, C. Toscano, and V. Lopresto, *A joint numerical-experimental study on impact induced intra-laminar and inter-laminar damage in laminated composites.* Applied Composite Materials, 2016. **23**(3): p. 219-237.

7. Flynn, E.B., M.D. Todd, P.D. Wilcox, B.W. Drinkwater, and A.J. Croxford. *Maximum-likelihood estimation of damage location in guided-wave structural health monitoring*. in *Proceedings of the Royal Society of London A: Mathematical, Physical and Engineering Sciences*. 2011. The Royal Society.

8. Tabtabaeipour, M., J. Hettler, S. Delrue, and K. Van Den Abeele. *Reconstruction Algorithm for Probabilistic Inspection of Damage (RAPID) in Composites*. in *11th European Conference on Non-Destructive Testing (ECNDT 2014)*. 2014.

9. Boccardi, S., D.-B. Calla, G.-P.M. Fierro, F. Ciampa, and M. Meo. *Nonlinear damage detection and localization using a time domain approach*. in *SPIE Smart Structures and Materials+ Nondestructive Evaluation and Health Monitoring*. 2016. International Society for Optics and Photonics.

10. Fierro, G.M., F. Ciampa, D. Ginzburg, E. Onder, and M. Meo, *Nonlinear ultrasound modelling and validation of fatigue damage.* Journal of Sound and Vibration, 2015. **343**: p. 121-130.

11. Ciampa, F., G. Scarselli, S. Pickering, and M. Meo, *Nonlinear elastic wave tomography for the imaging of corrosion damage.* Ultrasonics, 2015. **62**: p. 147-155.

12. Ciampa, F., G. Scarselli, and M. Meo, *Nonlinear imaging method using second order phase symmetry analysis and inverse filtering.* Journal of Nondestructive Evaluation, 2015. **34**(2): p. 1-6.

13. Ciampa, F., E. Barbieri, and M. Meo, *Modelling of multiscale nonlinear interaction of elastic waves with three-dimensional cracks.* The Journal of the Acoustical Society of America, 2014. **135**(6): p. 3209-3220.

14. Fierro, G.P.M. and M. Meo, *Nonlinear imaging (NIM) of flaws in a complex composite stiffened panel using a constructive nonlinear array (CNA) technique.* Ultrasonics, 2017. **74**: p. 30-47.

15. Ostrovsky, L. and P. Johnson, *Dynamic nonlinear elasticity in geomaterials.* Rivista del nuovo cimento, 2001. **24**(7): p. 1-46.

16. Guyer, R.A. and P.A. Johnson, *Nonlinear mesoscopic elasticity: Evidence for a new class of materials.* Physics today, 1999. **52**: p. 30-36.

17. Ciampa, F., S. Pickering, G. Scarselli, and M. Meo. *Nonlinear damage detection in composite structures using bispectral analysis*. in *SPIE Smart Structures and Materials+ Nondestructive Evaluation and Health Monitoring*. 2014. International Society for Optics and Photonics.

18. Ciampa, F., S.G. Pickering, G. Scarselli, and M. Meo, *Nonlinear imaging of damage in composite structures using sparse ultrasonic sensor arrays.* Structural Control and Health Monitoring, 2016.